Observation of polychromatic vortex solitons

Dragomir N. Neshev,[1,*] Alexander Dreischuh,[1,2] Vladlen Shvedov,[1,3] Anton S. Desyatnikov,[1] Wieslaw Krolikowski,[1] and Yuri S. Kivshar[1]

[1]*Nonlinear Physics Center and Laser Physics Center, Research School of Physical Sciences and Engineering, Australian National University, Canberra ACT 0200, Australia*
[2]*Department of Quantum Electronics, Sofia University, Sofia-1164, Bulgaria*
[3]*Department of Physics, Taurida National University, Simferopol 95007 Crimea, Ukraine*
[*]*Corresponding author: dnn124@rsphysse.anu.edu.au*

Received April 24, 2008; revised June 29, 2008; accepted July 3, 2008;
posted July 14, 2008 (Doc. ID 95379); published August 8, 2008

We demonstrate experimentally the formation of polychromatic single- and double-charge optical vortex solitons by employing a lithium niobate crystal as a nonlinear medium with defocusing nonlinearity. We study the wavelength dependence of the vortex core localization and observe self-trapping of polychromatic vortices with a bandwidth spanning over more than 70 nm for single-charge and 180 nm for double-charge vortex solitons. © 2008 Optical Society of America

OCIS codes: 190.4420, 190.6135, 260.6042.

The suppression of natural diffraction of light due to nonlinear self-focusing is a fascinating phenomenon that may lead to the formation of spatial optical solitons [1]. In defocusing nonlinear media both nonlinearity and diffraction contribute to the spreading of finite-size beams. As such, the formation of bright solitons is inhibited, but self-trapping of "dark filaments" can be observed instead [2]. This type of self-trapping leads to the formation of dark solitons, entities well-known in the context of nonlinear optics and Bose–Einstein condensates [1]. A dark soliton localized in two dimensions inherently carries an *optical vortex* (OV)—an isolated defect of the wavefront with a singularity of its phase and a twisted power flow [3]. While single-wavelength vortex solitons have been routinely observed, the experimental realization of the *multicolor* vortex solitons remains an experimental challenge. Only two-color simultaneous trapping of parametrically interacting optical vortices have been predicted and observed so far to our knowledge [4,5].

Simultaneous trapping of many chromatic components requires their incoherent interaction via cross-phase modulation in a Kerr-type medium. Such multifrequency trapping appears similar to the trapping of mutually incoherent modes of partially coherent light [6] but with the important difference that the polychromatic beam is spatially coherent and possesses a well-defined phase structure. While mutual trapping of many spatially incoherent vortex components at a single wavelength was observed a decade ago [7], to our knowledge so far the trapping of an optical vortex consisting of many spectral components has never been realized. The major obstacle is the chromatic dispersion present in the various techniques for vortex generation, leading to spatial separation of individual vortex colors. Chromatic effects near the core of a spatially coherent polychromatic vortex were predicted [8] and recently observed for "white-light" [9] and "rainbow" [10] vortex beams, as well as for ultrashort pulse vortices [11]. In addition, the spin-orbit coupling in uniaxial crystals has also been successfully implemented to generate white-light partially coherent vortices of single [12] and double [13] charges.

In this Letter we demonstrate, for the first time to our knowledge, the formation of spatially coherent white-light single- and double-charge optical vortex solitons. The broadband vortices are generated by a uniaxial potassium titanium oxide phosphate (KTP) crystal [12,13] onto a supercontinuum (SC) white-light beam that propagates in a lithium niobate ($LiNbO_3$) crystal. We show that the *defocusing nonlinearity* of the $LiNbO_3$ leads to mutual trapping of colors in the spectral window of 70 nm for single- and 180 nm for double-charge vortex solitons.

In our experiments we use a SC coherent white-light source in the spectral range of 450–700 nm. The Gaussian SC beam is converted to a polychromatic optical vortex (single or double charge) by a set of achromatic (450–800 nm) $\lambda/4$ wave plates, microscope objectives, a 7 mm long KTP crystal, and a polarizer (P) as shown in Fig. 1. When the SC beam propagates along the optical axis of the uniaxial KTP crystal, the scheme in Fig. 1 generates a *double-charge* optical vortex structure as described earlier [13]. If the quarter-wave plates, however, are removed and the polarizer (P) is set parallel to the polarization of the input beam, we generate a topological quadrupole of OVs. From this quadrupole, we isolate a *single-charge* OV by an iris diaphragm and tilting of the optical axis of the KTP crystal [12] at approximately 5°. The generated vortex beam is sub-

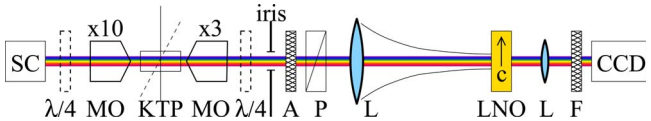

Fig. 1. (Color online) Experimental setup: SC, supercontinuum light source; $\lambda/4$, quarter-wave plates (not used for generation of a single charge OV); A, attenuator; MO, microscope objectives; L, lenses; P, polarizer; F, variable spectral filter; KTP, potassium titanium oxide phosphate (with adjustable tilting); LiNbO, lithium niobate crystals.

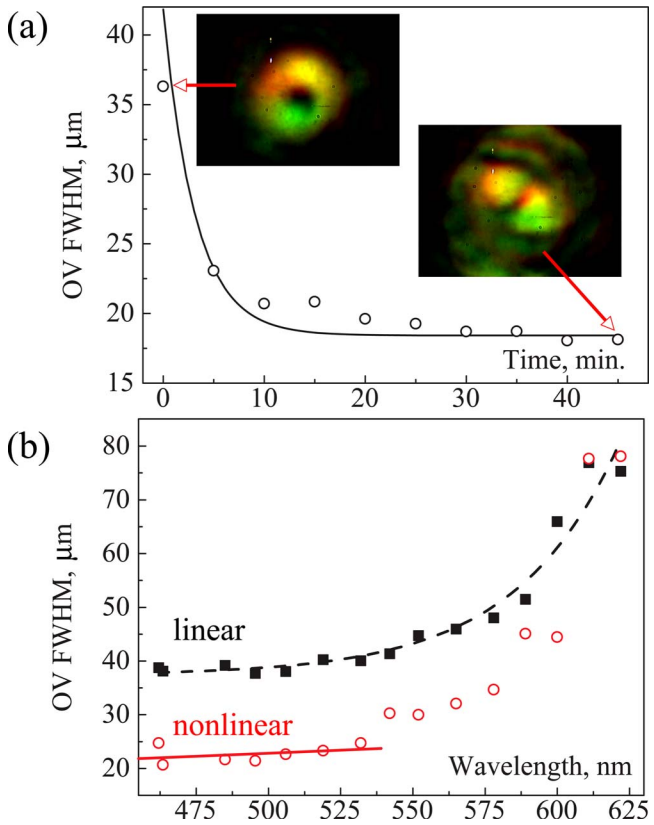

Fig. 2. (Color online) (a) Dependence of the average (over the azimuthal coordinate) core width of a single-charge polychromatic OV versus time (input power ~50 μW). Inset, output vortex intensity distribution in the linear (left) and nonlinear (right) regimes. (b) Width of the OV cores for different spectral components in linear (solid squares, dashed curve) and nonlinear (open circles) regimes. The solid curve indicates the wavelength range of the polychromatic OV soliton.

sequently attenuated by neutral density filters (A) and focused by an achromatic lens (f=120 mm) on the front facet of a 15-mm-long Fe-doped $LiNbO_3$ crystal. The polarization of the SC beam is set along the optical c axis of the crystal to maximize the photorefractive nonlinear response. An additional achromatic lens is used to image the input or output crystal facets onto a color CCD camera. A variable (300–750 nm) spectral filter (F) is used in front of the camera for selection of different spectral components.

First, we generate a single-charge polychromatic OV. Its intensity distribution at the exit of the $LiNbO_3$ crystal, just after the light beam has been turned on (total power ~50 μW), is shown in the left inset in Fig. 2(a). Owing to the slow nonlinear response of the crystal this initial distribution corresponds to a purely linear propagation regime. Images of the polychromatic OVs are subsequently recorded in 5 min intervals to measure the core FWHM (averaged over the azimuthal coordinate) as a function of time [Fig. 2(a)]. It is evident that the core of the vortex beam exhibits clear localization with time, reaching a steady state after approximately 25 min. This twofold decrease in size, from approximately 36 μm down to 18 μm (below the size of 24 μm at the input) is a strong indication for the formation of a polychromatic optical vortex soliton. On the other hand, the relatively complex coloring of the intensity distribution at the end of the observation period [see Fig. 2(a), right inset] indicates that the spectral components of the polychromatic vortex experience different nonlinear behavior. This difference is seen in Fig. 2(b) where we compare the linear (solid squares, dashed curve) and nonlinear (open circles) OV FWHM for different spectral components.

From this experimental data one can see that only short wavelength components of the polychromatic vortex are actually localized. This means that the polychromatic vortex soliton is generated only in the wavelength range 460–532 nm. The spatial localization becomes weaker with increasing the wavelength and approaches the linear diffraction size at 622 nm. This difference in the spectral localization is due to two major factors. First, the sensitivity of photorefractive nonlinearity of the $LiNbO_3$ crystal is strongly dependent on the wavelength [14]. The strongest contribution to the nonlinearity comes from the blue spectral components, which also experience the weakest diffraction. The red components, on the other hand, diffract much stronger and, therefore, they experience weaker localization.

The more important reason for a lack of the vortex core localization at long wavelengths, however, is the spatial dispersion of the OV core positions. The difference in spatial positions of the OV spectral components [12] is due to the dispersion in the tilted KTP crystal, causing the OV cores at different wavelengths to enter the nonlinear medium with a spatial offset. This offset is seen in Fig. 3 (top graph) demonstrating a linear spread of the OV spectral components of 15 and 25 μm in the x and y directions, respectively.

As seen in the bottom graph of Fig. 3, nonlinearity gradually decreases the OV core spreading along the crystalline c axis; however, the spreading in the per-

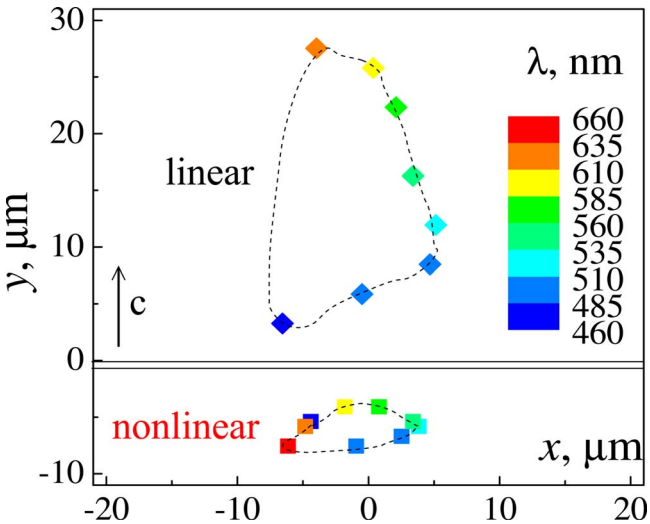

Fig. 3. (Color online) Transverse coordinates of the vortex cores at different spectral components in the linear and nonlinear regime. Owing to charge diffusion inside the $LiNbO_3$ crystal, the output vortex positions in the linear and nonlinear regimes are shifted by 120 μm along the direction of the c axis.

pendicular direction remains nearly unaffected. This spreading suppression is somewhat analogous to the self-trapping of bright incoherent vortices in self-focusing media [15], but it is strongly affected by the anisotropy of the photovoltaic nonlinearity.

Next, we study the formation of higher-charge localized structures, namely, double-charge vortex solitons. We note that such higher-charge OVs are nongeneric, and even a weak intensity perturbation causes vortex core splitting. Importantly, however, the experimental scheme for the generation of double-charge polychromatic OVs [13] does not require tilting of the KTP crystal and any possible vortex splitting remains smaller than the input size of the vortex core of approximately 72 μm. Furthermore, in contrast to the case of a single-charge OV, now all OV spectral components overlap inside the $LiNbO_3$ crystal. Owing to this overlap, the bandwidth for generation of a double-charge OV is determined solely by the achromaticity of the $\lambda/4$ wave plates.

The graph in Fig. 4 shows the double-charge OV core FWHM for the different spectral components. The vortex size is measured for both linear (few nanowatts input power) and nonlinear ($\sim$50 μW input power) regimes. We observe linear diffraction of the different spectral components (solid squares, dashed curve) with the vortex-core size increasing monotonically with wavelength. Surprisingly, in the nonlinear regime all OV spectral components are mutually trapped at the crystal output and localized to the same size of approximately 122 μm. This result demonstrates a successful formation of a polychromatic double-charge OV soliton of more than 180 nm spectral bandwidth.

It is worth mentioning that if the polychromatic OV beam remains in the crystal for more than 3 h or the input power is increased, resulting in stronger

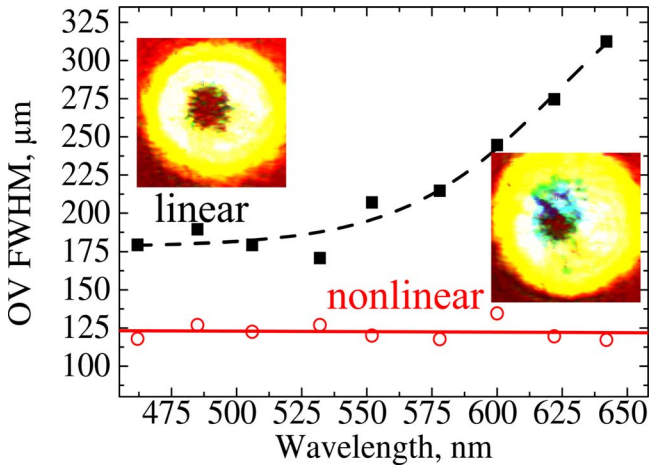

Fig. 4. (Color online) Optical vortex width at individual spectral components in the linear (solid squares) and nonlinear (open circles) regimes of polychromatic double-charged OV soliton formation. Insets, output intensity distributions in the two regimes.

nonlinear response, we observe a double-charge OV spliting in two well-distinguished single-charge OVs. This splitting is due to the intrinsic higher-charge nonlinear vortex instability [16,17] and prevents the narrower localization of the vortex core at the output.

In conclusion, we have demonstrated that single- and double-charge polychromatic OV solitons can be generated in defocusing photorefractive nonlinear media due to the nonlinear interaction between all spectral components. We have observed that the nonlinear self-action in the $LiNbO_3$ crystal leads to significant vortex core confinement for both single- and double-charge OV solitons and to a reduction of the positional spread in the single-charge OV spectral components. Our findings reveal that the physical nature of the polychromatic vortex solitons is defined not merely as a sum of monochromatic vortex solitons, but by the mutual incoherent trapping of all OV spectral components.

This work was supported by the Australian Research Council through Discovery and Linkage International projects and by the National Science Foundation (NSF)-Bulgaria, project WUF-02/05.

References

1. Yu. S. Kivshar and G. P. Agrawal, *Optical Solitons: From Fibers to Photonic Crystals* (Academic, 2003).
2. G. A. Swartzlander, Jr. and C. T. Law, Phys. Rev. Lett. **69**, 2503 (1992).
3. A. S. Desyatnikov, Yu. S. Kivshar, and L. Torner, in *Progress in Optics*, E. Wolf, ed. (North-Holland, 2005), Vol. 47, and references therein.
4. T. J. Alexander, A. V. Buryak, and Yu. S. Kivshar, Opt. Lett. **23**, 670 (1998).
5. P. Di Trapani, W. Chinaglia, S. Minardi, A. Piskarskas, and G. Valiulis, Phys. Rev. Lett. **84**, 3843 (2000).
6. M. Mitchell and M. Segev, Nature **387**, 880 (1997).
7. Z. Chen, M. Mitchell, M. Segev, T. H. Coskun, and D. N. Christodoulides, Science **280**, 889 (1998).
8. M. Berry, New J. Phys. **4**, 66 (2002).
9. J. Leach and M. J. Padgett, New J. Phys. **5**, 154 (2003).
10. M. S. Soskin, P. V. Polyansky, and O. O. Arkheluyk, New J. Phys. **6**, 196 (2004).
11. K. Bezuhanov, A. Dreischuh, G. G. Paulus, M. G. Schätzel, and H. Walther, Opt. Lett. **29**, 1942 (2004).
12. A. Volyar, V. Shvedov, T. Fadeyeva, A. S. Desyatnikov, D. N. Neshev, W. Krolikowski, and Yu. S. Kivshar, Opt. Express **14**, 3724 (2006).
13. V. Shvedov, W. Krolikowski, A. Volyar, D. N. Neshev, A. S. Desyatnikov, and Yu. S. Kivshar, Opt. Express **13**, 7393 (2005).
14. D. N. Neshev, A. A. Sukhorukov, A. Dreischuh, R. Fischer, S. Ha, J. Bolger, L. Bui, W. Krolikowski, B. J. Eggleton, A. Mitchell, M. W. Austin, and Yu. S. Kivshar, Phys. Rev. Lett. **99**, 123901 (2007).
15. C. C. Jeng, M. F. Shih, K. Motzek, and Yu. S. Kivshar, Phys. Rev. Lett. **92**, 043904 (2004).
16. A. V. Mamaev, M. Saffman, and A. A. Zozulya, Phys. Rev. Lett. **77**, 4544 (1996).
17. A. Dreischuh, G. G. Paulus, F. Zacher, F. Grasbon, D. Neshev, and H. Walther, Phys. Rev. E **60**, 7518 (1999).